

Received: 2019.12.03

Accepted: 2020.02.03

Available online: 2020.03.31

Published: 2020.05.30

Hirudin Reduces the Expression of Markers of the Extracellular Matrix in Renal Tubular Epithelial Cells in a Rat Model of Diabetic Kidney Disease Through the Hypoxia-Inducible Factor-1 α (HIF-1 α)/Vascular Endothelial Growth Factor (VEGF) Signaling Pathway

Authors' Contribution:

Study Design A
Data Collection B
Statistical Analysis C
Data Interpretation D
Manuscript Preparation E
Literature Search F
Funds Collection G

AG 1 **Xinxin Pang**
CE 2 **Yage Zhang**
B 2 **Xiujie Shi**
B 2 **Zining Peng**
CF 2 **Yufeng Xing**
DG 2 **Jiarui Han**

1 Department of Nephropathy, Henan Provincial Hospital of Traditional Chinese Medicine, Zhengzhou, Henan, P.R. China
2 Henan University of Chinese Medicine, Second Clinical Medical College, Zhengzhou, Henan, P.R. China

Corresponding Author: Jiarui Han, e-mail: Hanjr2018@126.com

Source of support: This study was funded by the Research Project of the National TCM Clinical Research Base (No. 2019JDZX068); the Special Research Project of TCM in Henan Province (2019ZYBJ17); A Sub-Station Project of the Inheritance Studio of Famous Old Chinese Medicine Experts Across the Country; TCM Top Talent Training Project of Henan Province; National TCM Innovational Core Talent Training Project

Background: This study aimed to investigate the effects of hirudin on the production of extracellular matrix (ECM) factors by renal tubular epithelial cells in a rat model of diabetic kidney disease (DKD) and HK-2 human renal tubule epithelial cells.





Material/Methods: Sprague-Dawley rats were divided into the normal control group (n=10), the normal control+hirudin group (n=10), the DKD model group (n=12) and the DKD+hirudin group (n=12). At the end of the study, renal histopathology was undertaken, and the expression of type IV collagen, fibronectin, hypoxia-inducible factor-1 α (HIF-1 α), and vascular endothelial growth factor (VEGF) were evaluated using immunohistochemistry, Western blot, and quantitative real-time polymerase chain reaction (qRT-PCR). HK-2 cells were cultured in glucose and treated with hirudin. Protein and mRNA expression of fibronectin, type IV collagen, HIF-1 α , and VEGF were evaluated following knockdown or overexpression of HIF-1 α .

Results: Hirudin significantly improved renal function in the rat model of DKD (P<0.01), and significantly down-regulated the expression of fibronectin, type IV collagen, HIF-1 α , and VEGF proteins (P<0.05). The expression of ECM associated proteins was increased in HK-2 cells treated with high glucose and reduced in the high glucose+shRNA HIF-1 α group (P<0.05). Compared with the control group, the expression of ECM associated proteins was increased in the HIF-1 α over-expressed group, and decreased following treatment with hirudin (P<0.05).

Conclusions: Hirudin reduced the expression of markers of ECM by inhibiting the HIF-1 α /VEGF signaling pathway in DKD renal tubular epithelial cells.

MeSH Keywords: **Diabetic Nephropathies • Extracellular Matrix • Hirudins • Hypoxia-Inducible Factor 1 • Vascular Endothelial Growth Factors**

Full-text PDF: <https://www.medscimonit.com/abstract/index/idArt/921894>

 3646  2  6  27



Background

Diabetic kidney disease (DKD) is a potentially life-threatening microvascular complication of type 1 and type 2 diabetes mellitus, and its incidence has nearly doubled in the past decade [1]. Between 10–30% of patients with diabetes are at increased risk of DKD [1]. Clinically, DKD is characterized by a progressively increasing albuminuria (>300 mg/day or >200 mcg/min) and a variable rate of decline in the glomerular filtration rate (GFR) [2]. The pathogenesis of DKD is characterized by significant structural changes in the kidney, including renal hypertrophy, glomerular ultrafiltration, mesangial dilatation, and thickening of the glomerular basement membrane (GBM) due to increased deposition of extracellular matrix (ECM) components, including collagen I, IV, and fibronectin. Structural and functional changes in glomerular cells also adversely affect the cells lining the renal tubules, leading to glomerular sclerosis and tubulointerstitial fibrosis, which results in end-stage renal disease (ESRD) [2]. Currently, DKD has no treatment and approaches to improve renal function and patient prognosis are required [3,4].

Recently, the role of renal tubular fibrosis has been recognized to have a main role in the progression of DKD and is an indicator of poor patient prognosis [5]. Studies have shown that the deposition of ECM is an important mechanism in renal tubular fibrosis associated with DKD [6,7]. Chronic hyperglycemia drives the formation and accumulation of the ECM proteins that lead to renal tubular fibrosis, and therapeutic strategies that target renal fibrosis are needed in the management of DKD [6,7].

Hirudin is a naturally occurring thrombin inhibitor and a potent anticoagulant. The hirudin molecule is a 65 amino acid polypeptide with a molecular weight of approximately 7000 Da [8]. Hirudin is derived from the salivary glands of medicinal leeches, including *Hirudo medicinalis*, which has been used in traditional Chinese medicine to promote blood circulation and is often used in the treatment of DKD [8]. Previous studies have shown that hirudin inhibits myocardial fibrosis [9]. However, there have been no previous studies on the effects of hirudin on renal fibrosis in DKD. Therefore, this study aimed to investigate the effects of hirudin on the production of extracellular matrix (ECM) factors by renal tubular epithelial cells in a rat model of diabetic kidney disease (DKD) and HK-2 human renal tubule epithelial cells.

Material and Methods

Experimental animals

Fifty male Sprague-Dawley rats, 8 weeks of age, with a mean body weight of 150 ± 10 g, were obtained from the Henan Experimental Animal Center, University of Chinese Medicine (Certificate No: SCXK [Yu] 2017-0001) and allowed to acclimate for one week. The animals were housed in groups of three in laboratory cages under controlled laboratory conditions at a temperature of $23\pm 2^\circ\text{C}$, and relative humidity of 40–50% with a 12-hourly light and dark cycle and were given *ad libitum* access to a standard diet and tap water. All the rats were healthy and had no infection during the experimental period. Before the study began, the blood glucose was normal, and the urine protein test was negative for all the animals. The animals were cared for according to The Guide for the Care and Use of Laboratory Animals in China, and the study was approved by the Ethics Committee of the Henan Provincial Hospital of Traditional Chinese Medicine.

Twenty rats were randomly divided into the normal control group (n=10) and the normal control+hirudin group (n=10). The remaining 30 rats were used to develop the experimental model of diabetes mellitus that was induced with an intraperitoneal injection of streptozotocin (STZ) (55 mg/kg), which was freshly prepared in citrate buffer (pH=4.5). The rats were treated with STZ under fasting conditions. The normal control group and the normal control+hirudin group were injected with an equal volume of citrate buffer [10]. At 72 hours following injection, the blood glucose level of the rats was measured. Rats with blood glucose levels ≥ 16.7 mmol/L on three consecutive measurements were confirmed to represent the model of diabetes mellitus. Of the 30 rats, 28 had high blood glucose. The 24-hour urine protein was measured after eight weeks. A urine protein was ≥ 30 mg/L confirmed the successful establishment of the DKD model, which was established in 24 rats [11]. The 24 rats in the established DKD model were randomly divided into the model group (n=12) and the DKD+hirudin group (n=12). The normal control+hirudin group and the DKD+hirudin group were subcutaneously injected with hirudin (1 ATU) [12]. Rats in the normal control group and the model group were subcutaneously injected with normal saline of 1mg/kg/d. Hirudin was administered daily for 16 weeks. All rats were euthanized humanely after 16 weeks of treatment with or without hirudin.

Cell culture

Human immortalized renal tubular epithelial (HK-2) cells were purchased from the American Type Culture Collection (ATCC) (Manassas, VA, USA). HK-2 cells were cultured in F12 Dulbecco's modified Eagle's medium (DMEM) supplemented with 10% fetal

bovine serum (FBS) (Invitrogen, Carlsbad, CA, USA), 100 U/ml penicillin and streptomycin in a humidified atmosphere of 5% CO₂ at 37°C. Before treatment, the cells were cultured to between 80–90% confluence. HK-2 cells were then treated with hirudin 10 mg/mL (Guangxi Kekang Natural Water Purification Institute, China) (Cat. No.: ZL03113566.8) [13].

Blood glucose and renal function testing

During the 16 week period after the development of the rat model, blood glucose levels were measured every four weeks, using an Abbott glucose meter (Abbott Labs, Abbott Park, Ill, USA). An albumin assay kit (Nanjing Institute of Bioengineering, China; A028-1-1), the 24-hour urine protein content was determined. Rats were weighed and fasted for 12 h before they were euthanized. Blood samples were also collected from the aorta when the rats were under 10% chloral hydrate anesthesia. The blood samples were centrifuged at 3,000 rpm for 10 min, and the serum was separated. Blood urea nitrogen (BUN) was measured using a urea nitrogen assay kit (C011-1-1) and serum creatinine was measured using a creatinine assay kit (C013-1-1) (Nanjing Jiancheng Bioengineering Institute, Nanjing, China) to assess renal function.

Renal histopathology

Histology of the rat kidneys was performed to assess the diabetic changes in the renal glomeruli. The kidney tissue samples were harvested, fixed in 4% paraformaldehyde, and embedded in paraffin wax. Tissue sections were cut at 4 µm onto glass slides and stained histochemically with hematoxylin and eosin (H&E), Masson's trichrome, and periodic acid–Schiff (PAS). The renal tissue sections were examined by light microscopy.

Western blot

Samples of the renal cortex or HK-2 cells were harvested, washed, and total proteins were extracted in ice-cold RIPA buffer containing protease and phosphatase inhibitors (Sigma-Aldrich, St. Louis, MO, USA). Protein concentrations were quantified using a BCA protein assay kit (KeyGen Biotech Co. Ltd., Nanjing, China). Western blot was performed with equal amounts of protein separated by electrophoresis on 12% sodium dodecyl sulfate-polyacrylamide gel electrophoresis (SDS-PAGE) gel and transferred to a nitrocellulose membrane. The membranes were incubated with 5% dried skimmed milk powder in tris-buffered saline (TBS). The membranes were incubated with primary antibodies to β-actin (Cat. No. 60008-1-Ig; Proteintech, Manchester, UK), type IV collagen (ab6586; Abcam, Cambridge, MA, USA), fibronectin (ab45688; Abcam, Cambridge, MA, USA), hypoxia-inducible factor-1α (HIF-1α) (20960-1-AP; Proteintech, Manchester, UK), vascular endothelial growth factor (VEGF) (66828-1-Ig; Proteintech,

Manchester, UK). The membranes were washed twice with TBST and incubated with secondary antibodies conjugated with horseradish peroxidase (HRP) (1: 2000) for 1 hour at room temperature. The bands on the membranes were observed with electrochemiluminescence (ECL) reagent (Amersham, Uppsala, Sweden), and grayscale imaging was performed using ImageJ software (National Institutes of Health, Bethesda, MD, USA) and normalized with GAPDH (1: 1500) as the internal control.

Quantitative real-time polymerase chain reaction (qRT-PCR)

Total RNA from mouse kidney tissues or HK-2 cells was extracted using TRIzol reagent (Invitrogen, Carlsbad, CA, USA), and cDNA was synthesized using the Superscript™ First-Strand cDNA Synthesis System (Invitrogen, Carlsbad, CA, USA), according to the manufacturer's instructions. The qRT-PCR assay was performed using the Power SYBR Green Master Mix kit (Thermo Fisher Scientific, Waltham, MA, USA) on an ABI Prism 7000 sequence detection system (Applied Biosystems, Foster City, CA, USA). The qRT-PCR cycle profile was performed at 94°C for 5 min, followed by 40 cycles of 15s and 30s at 94°C with a denaturation temperature, 30s at annealing temperatures of 55°C and 30s at 72°C for the final extension, with β-actin as an internal reference. The relative mRNA level fold change was calculated using the 2^{-ΔΔCT} method. The primers used are listed in Table 1.

Immunohistochemistry

The kidney tissue was fixed in 4% paraformaldehyde and embedded in paraffin wax. Tissue sections were cut at 5 µm, dewaxed, and then washed three times with PBS for 5 minutes. The tissue sections were incubated in 1% Triton X-100 and 3% hydrogen peroxide solution for 10 minutes [10]. The tissue sections were blocked with 5% goat serum in PBS for 30 min and incubated overnight at 4°C with primary antibodies against type IV collagen (1: 200), fibronectin (1: 200), HIF-1α (1: 100), and VEGF (1: 100). After washing three times with TBS for 5 min, the tissue sections were incubated with HRP-conjugated anti-rabbit IgG secondary antibody (Amersham, Arlington Heights, IL, USA) for 30 min at 37°C. Then, 50 µl of 3,3'-diaminobenzidine (DAB) substrate solution (Sigma-Aldrich, St. Louis, MO, USA) was added to the tissue sections and incubated for 10 min at room temperature. The tissue sections were rinsed three times with PBS, and counterstained with Mayer's hematoxylin for 6–10 min, dehydrated, and examined using a light microscope.

Cell proliferation assay

Cell viability was assessed using the Cell Counting Kit-8 (CCK8) assay (Dojindo Laboratories, Kumamoto, Japan), according to

Table 1. The primer sequences used.

Gene	Species	Sequences of the primers
HIF-1 α	Rat	Forward: 5'-CTCCCTTTTCAAGCAGCAG-3' Reverse: 5'-CAGGTGTTTCTGGGTAGGC-3'
	Human	Forward: 5'-GTTACCTGAGCCTA ATAGTCC-3' Reverse: 5'-GGAACGTAAGTGGAGTCATC-3'
Type IV collagen	Rat	Forward: 5'-CCTGGGCAGATTCCAAACCT-3' Reverse: 5'-CAAAGGCGTCGTCAATCACC-3'
	Human	Forward: 5'-AAGACCTGGTACTCTGGGC-3' Reverse: 5'-AGTAATTGGGGCCATGTCCA-3'
Fibronectin	Rat	Forward: 5'-GTTGGTTGCCCTGTTCTGC-3' Reverse: 5'-GGCTACCTGTGTTCCCTTTG-3'
	Human	Forward: 5'-AAAACCTCAGGAAACTC-3' Reverse: 5'-GTGCGACACTATTCTATTTC-3'
VEGF	Rat	Forward: 5'-GCACCCATGGCAGAAGG-3' Reverse: 5'-CTCGATTGGATGGCAGTAGCT-3'
	Human	Forward: 5'-TGCTAGATCTCCAGAGAT-3' Reverse: 5'-TCGTGCATATGTGCTTCTAC-3'
β -actin	Rat	Forward: 5'-CGCCCAGCAGATGAAA-3' Reverse: 5'-CCGCCGATCCACACAGA-3'
	Human	Forward: 5'-CATGTACGTTTGTATCCAGGC-3' Reverse: 5'-CTCCTTAATGTCACGCACGAT-3'

the manufacture's protocol. Briefly, HK-2 cells were seeded into a 96-well culture plate at a density of 3×10^4 cells/ml. Following different treatments, 10 μ l of CCK-8 reagent was added to each well and the cells were incubated for 4 h at 37°C. Cell viability was determined by measuring the optical density (OD) at an absorbance of 490 nm with a microplate reader [13].

Cell transfection

HIF-1 α shRNA and pcDNA-HIF-1 α were obtained from GenePharma (Shanghai, China). The shRNA sequence was: HIF-1 α shRNA: 5'-GAAACTCTCCAAGCAATTTT-3'. The transfection mixture was incubated at room temperature, and the cells were harvested in RPMI 1640, supplemented with 10% FBS without antibiotics. In total, 10^5 HK-2 cells per well were mixed with the transfection mixture followed by the addition of 1 ml of antibiotic-free growth medium, and incubated overnight. On the following day, the supernatant was replaced by 2 ml of fresh antibiotic-free growth medium. The cells were harvested after 48 h for further analysis.

The recognized gene fragment of the HIF-1 α gene was extracted from the pEGFP-N1-HIF-1 α vector plasmid, and the restriction site sequence was added upstream and downstream. The 5' end upstream was the BamHI restriction site sequence and the 3' downstream sequence of the Ascl restriction site.

The specific primers were:

forward: 5'-AGCACGACTTGATTTTCTCCC-3';
reverse: 5'-TTCTTGATTGAGTGCAGGGT-3'.

According to the manufacturer's instructions for the lentivirus kit, 24 h before transfection, HK-2 cells in good condition and the logarithmic growth phase were inoculated into a 10 cm cell culture dish, and cultured in 5% CO₂ at a temperature of 37°C, until the cell density reached 70–80% for transfection. Transfection was performed in strict accordance with the instructions for the lentivirus packaging kit (Thermo Fisher Scientific, Waltham, MA, USA). After 6 h post-transfection, the medium was replaced with fresh DMEM containing 0.5% BSA. Following 6–8 h of incubation, the cells were harvested for further analysis.

Statistical analysis

Statistical analysis was performed using SPSS version 19.0 software (IBM Corp., Armonk, NY, USA). All experiments performed in triplicate. Data from three or more independent experiments were expressed as the mean \pm standard deviation (SD). Data obtained from each group were tested by one-way analysis of variance (ANOVA). Differences between two groups were determined using Student's t-test. A P-value <0.05 was considered to be statistically significant.

Table 2. The effects of hirudin on fasting blood glucose, 24 h-urinary protein, creatinine, and urea nitrogen in the rat model of diabetic kidney disease (DKD).

Group	Blood glucose (mmol/L)	Serum creatinine (μmol/L)	Blood urea nitrogen (mmol/L)	24 h urinary protein (mg/L)
Ctrl	7.07±0.90	61.30±4.52	6.03±1.25	4.52±0.78
STZ	22.69±3.49 ^{##}	77.27±1.57 ^{##}	16.63±2.38 ^{##}	36.96±1.47 ^{##}
STZ+H	18.56±1.56 ^{**}	66.08±2.22 ^{**}	9.13±1.30 ^{**}	20.99±2.85 ^{**}
Ctrl+H	7.16±0.91	61.19±4.55	6.07±1.17	4.57±0.91

STZ – streptozotocin; H – hirudin; Ctrl – control. Compared with the normal control group, ^{##} P<0.01; [#] P<0.05; compared with the model group, ^{**} P<0.01; ^{*} P<0.05.

Results

The effects of hirudin on proteinuria, renal function, and renal histology in the rat model of diabetic kidney disease (DKD)

Blood glucose, serum creatinine, 24 h urine protein, and urea nitrogen levels were measured to evaluate the effect of hirudin on renal function in the diabetic rat model. Compared with the normal group, blood glucose, serum creatinine, 24 h urine protein, and urea nitrogen levels in the DKD group were significantly higher than those in the normal control group (p<0.01) (Table 2), indicating that the model group had impaired kidney function. Hirudin treatment did not affect blood glucose, serum creatinine, 24 h urinary protein, and urea nitrogen in normal rats. However, significantly reduced blood glucose, serum creatinine, 24 h urinary protein, and urea nitrogen levels were observed in diabetic rats (p<0.01), indicating that hirudin reduced kidney damage and improved renal function in the diabetic rat model.

Histology of the rat kidney was performed using histochemical staining with hematoxylin and eosin (H&E), periodic acid-Schiff (PAS), and Masson's trichrome (Figure 1). Compared with normal renal tissues, rats in the model group showed mesangial stromal hyperplasia, mesangial cell proliferation, glomerular sclerosis, and vacuolar degeneration of the tubule epithelial cells in the model group (Figure 1A). The histological changes in the rat kidneys of the model+hirudin treated group were reduced when compared with the untreated model group, including the deposition of PAS-positive extracellular matrix (ECM) components (Figure 1B). The histology of the kidney tissue of the normal control group was showed no pathological changes. However, the renal tubular basement membrane in the model group showed varying degrees of deposition of PAS-positive material in the proximal convoluted tubule. The glomerular basement membrane (GBM) and renal tubular lesions in the model+hirudin group were reduced compared with the model group, and the amount of PAS-positive

staining material in the glomerular mesangium and tubulointerstitial renal tissue and the renal tubular epithelial cell lesions was significantly reduced. Masson's trichrome staining (Figure 1C) showed the deposition of collagen fibers in the glomeruli of the rats in the model. Collagen fibers were found in the interstitium of the model group, which was reduced in the hirudin treatment group.

The effect of hirudin on ECM in the rat model of DKD

Immunohistochemistry was performed on the renal tissue to assess the ECM accumulation in the rat model of DKD (Figure 2A, 2B). The findings showed increased levels of type IV collagen and fibronectin in the kidneys of the diabetic rats. Hirudin significantly reduced the levels of type IV collagen and fibronectin in the rat kidneys. Western blot and quantitative real-time polymerase chain reaction (qRT-PCR) showed that the protein expression of type IV collagen and fibronectin in the model group was higher than that in the normal group (Figure 3A–3E). The expression of type IV collagen and fibronectin were significantly down-regulated in the model+hirudin group compared with the model group (P<0.05). Quantitative real-time polymerase chain reaction (qRT-PCR) showed that the trends in mRNA expression supported the trends in protein expression.

The effects of hirudin on the hypoxia-inducible factor-1α (HIF-1α) and vascular endothelial growth factor (VEGF) pathway in the rat model of DKD

The expression of HIF-1α and VEGF in the model group were significantly increased compared with the normal control group. However, hirudin treatment reduced the expression of HIF-1α and VEGF (Figure 2C, 2D), which was supported by the findings from Western blot (Figure 4A–4E). Compared with the normal group, the expression of HIF-1α and VEGF in the model group were significantly increased (P<0.01). Hirudin treatment reduced the expression of HIF-1α and VEGF in the rat model

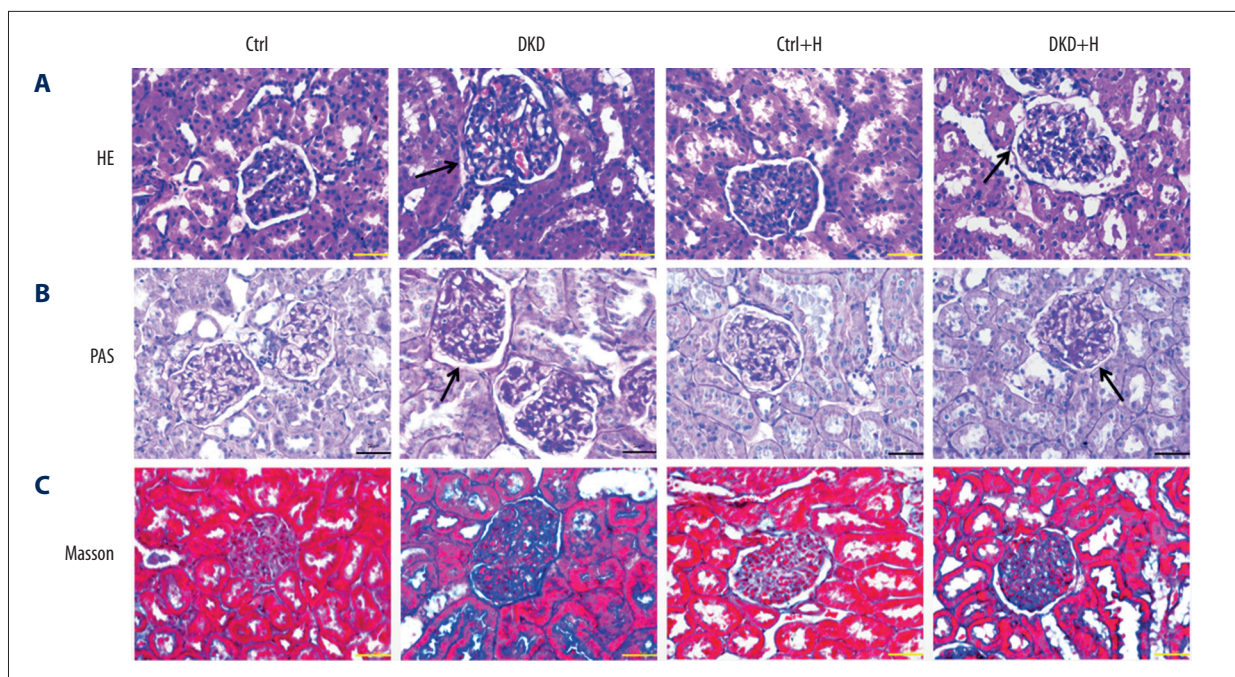


Figure 1. Photomicrographs of the histological changes in the kidney tissues from the study groups in the rat model of diabetic kidney disease (DKD). **(A)** Hematoxylin and eosin (H&E) staining shows that the histological changes in the renal tubules, glomerulus, and mesangial matrix in the model+hirudin group were reduced compared with the model group. The arrows in the figure indicate hyperplasia of the mesangial matrix. (Magnification $\times 400$). **(B)** Periodic acid Schiff (PAS) staining shows that the tubule basement membrane of the model group is thickened, the proximal tubules are dilated, and the tubules are dilated. The arrows indicate the deposition of PAS-positive material. (Magnification $\times 400$). **(C)** Masson's trichrome staining shows that collagen fibers are deposited in the glomeruli of the DKD rat model. The hirudin treatment group could reduce renal interstitial fibers. The blue substance is the deposition of collagen fibers. Ctrl – control; DKD – diabetic kidney disease; H – hirudin. Ctrl+H – normal control+hirudin group; DKD+H – DKD+hirudin group. Following the establishment of the DKD rat model, the normal control+hirudin group, the DKD+hirudin group were subcutaneously injected with hirudin (1 ATU). Rats in the normal control group and model group were subcutaneously injected with normal saline (1 mg/kg/day).

of DKD ($P < 0.05$). The qRT-PCR data showed that the trends in mRNA expression supported the trends in protein expression.

The effects of hirudin on the proliferation of HK-2 cells *in vitro*

The results of the Cell Counting Kit-8 (CCK-8) assay for the viability of HK-2 cells showed that hirudin significantly inhibited cell viability at 24 hours and 48 hours in a dose-dependent manner. The cell viability was lower than 50% when cells were treated with 160 $\mu\text{g}/\text{mL}$ and 320 $\mu\text{g}/\text{mL}$ of hirudin for 48 hours. Also, HK-2 cells were divided into the normal group, the high glucose group, and the hirudin+high glucose group. After 12 h, 24 h, and 48 h of intervention, the CCK-8 assay detected cell proliferation of each group and showed that HK-2 cells in the high glucose group reduced survival compared with the normal group. The cell survival rate of the hirudin+high glucose group was higher than that of the high glucose group, particularly after 24 h of intervention. Therefore, the partial intervention time for the *in vitro* study was determined to be 24 h (Figure 5).

The effects of hirudin on high glucose-induced ECM expression in HK-2 cells were mediated through the HIF-1 α /VEGF pathway

In this study, shRNA-HIF-1 α and pcDNA-HIF-1 α were used to investigate the effect of hirudin on ECM associated proteins and the HIF-1 α /VEGF pathway in HK-2 cells under conditions of high glucose. Compared with the high glucose group, HIF-1 α knockdown significantly reduced the levels of high glucose-induced ECM associated proteins, fibronectin, and type IV collagen in HK-2 cells (Figure 6A–6G). These findings indicated that inhibition of the HIF-1 α /VEGF pathway reduced ECM in HK-2 cells in conditions of high glucose. However, overexpression of HIF-1 α significantly upregulated the expression of the ECM associated proteins, fibronectin, and type IV collagen, which supported the role of the HIF-1 α /VEGF pathway in ECM deposition (Figure 6H–6N). Also, overexpression of HIF-1 α showed that treatment with hirudin significantly reduced the expression of fibronectin and type IV collagen, indicating that hirudin inhibited the HIF-1 α /VEGF pathway in ECM accumulation in HK-2 cells induced by high glucose levels.

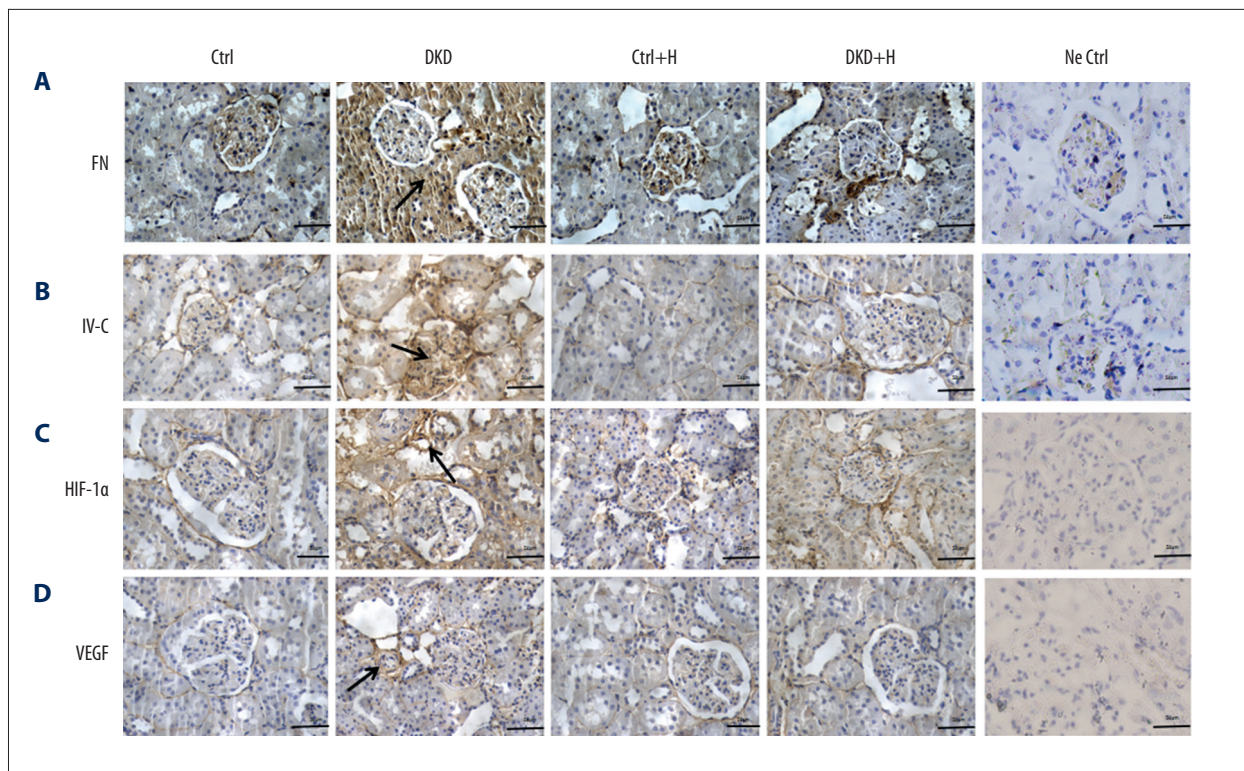


Figure 2. (A–D) Immunohistochemistry of markers of the extracellular matrix (ECM), hypoxia-inducible factor-1 α (HIF-1 α), and vascular endothelial growth factor (VEGF) in kidney tissue in the rat model of diabetic kidney disease (DKD). Immunohistochemical expression of ECM associated proteins, including fibronectin and type IV collagen, and hypoxia-inducible factor-1 α , and vascular endothelial growth factor (VEGF). (Magnification $\times 400$). The arrow indicates positive immunostaining. STZ – streptozotocin; Ne – negative; FN – fibronectin; IV-C – type IV collagen; HIF-1 α – hypoxia-inducible factor-1 α ; VEGF – vascular endothelial growth factor; Ctrl – control; DKD – diabetic kidney disease; H – hirudin. Ctrl+H – normal control+hirudin group; DKD+H –DKD+hirudin group.

Discussion

Diabetic kidney disease (DKD) is a progressive microvascular complication of diabetes mellitus and is the main cause of end-stage renal disease (ESRD) [14,15]. DKD is characterized by proteinuria and progressive deterioration of renal function [16]. Early histological changes include mesangial expansion, arteriolar hyaline deposition, tubulointerstitial extracellular matrix (ECM) deposition, progressive and advanced glomerular sclerosis, and renal interstitial fibrosis [17]. As clinical treatment for DKD remains clinically challenging, patients have to rely on dialysis or renal replacement therapy (RRT). Therefore, it is important to investigate new interventions and intervention targets.

Previously, DKD was considered to be a progressive disorder characterized by marked urinary microalbumin excretion and hyperfiltration, with glomeruli injury as the predominant mode of presentation, and with microalbuminuria used as a marker of kidney damage. However, recent clinical studies have identified a non-albuminuric phenotype as the predominant mode of DKD presentation. As renal tubular injury occurs at an earlier

stage than glomerular injury, renal tubular injury has been reported to be associated with the pathophysiology and prognosis of DKD [18,19]. Therefore, renal tubular injury represents a potential new target for interventions in DKD [2].

Previous studies have shown that high glucose-mediated tubulointerstitial accumulation of extracellular matrix (ECM) has an important role in the pathogenesis of DKD. The ECM is the driving factor for advanced fibrosis in DKD, involving several cells in the kidney, including glomerular endothelial cells, mesangial cells, podocytes, and renal tubular epithelial cells [2,20]. ECM contains mainly several types of collagen, including type I, II, III, and IV collagen, non-collagen glycoprotein, fibronectin, fibrillin, proteoglycans, and glycosaminoglycans that include chondroitin sulfate, and leucine-rich glycoproteins [21]. Increased deposition of ECM leads to tubulointerstitial fibrosis, which is the main cause of reduced renal function in DKD. Therefore, new treatment approaches may be directed to control ECM deposition in DKD.

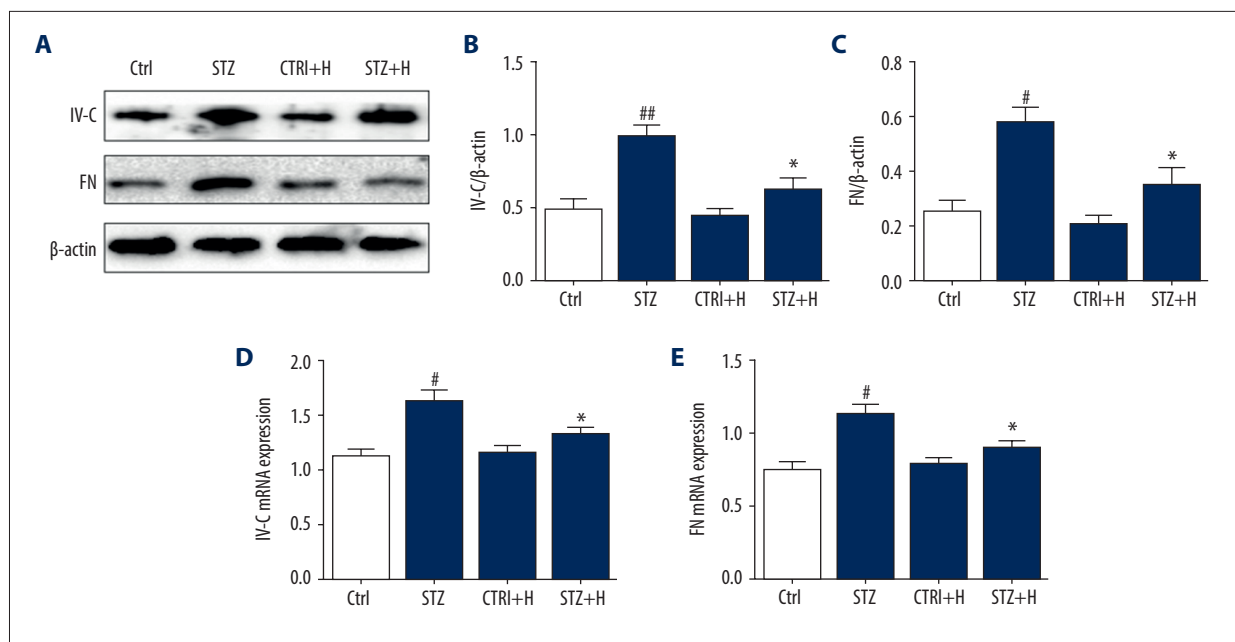


Figure 3. The effects of hirudin on the expression of fibronectin and type IV collagen in the rat model of diabetic kidney disease (DKD). **(A)** The protein expression levels of type IV collagen and fibronectin were determined by Western blot. **(B, C)** Quantification of protein expression was performed using GraphPad Prism version 7.0. β -actin was used as an internal control. The gray value was evaluated and calculated qualitatively. **(D, E)** The relative mRNA levels of type IV collagen, fibronectin was evaluated using quantitative real-time polymerase chain reaction (qRT-PCR). All data are expressed as the mean \pm standard deviation (SD). Compared with the normal control group, ^{##} $P < 0.01$; [#] $P < 0.05$. Compared with the model group, ^{**} $P < 0.01$; ^{*} $P < 0.05$. STZ – streptozotocin; DKD – diabetic kidney disease; H – hirudin; FN – fibronectin; IV-C – type IV collagen; HIF-1 α – hypoxia-inducible factor-1 α ; VEGF – vascular endothelial growth factor. Ctrl – control; Ctrl+H – the normal control+hirudin group; DKD+H –DKD+hirudin group.

Hirudin is an anticoagulant produced by the salivary glands of the medicinal leech. Previous studies have mainly focused on the anticoagulant and anti-inflammatory effects of hirudin and have shown that it can antagonize ECM deposition in different cell types [22,23]. Medicinal leeches have been used in traditional Chinese medicine in the treatment of DKD, and previous studies have shown that hirudin can inhibit fibrosis associated with cardiomyocytes [9]. However, the effect of hirudin in renal tubular ECM deposition in DKD has not previously been established [2]. This study was the first to investigate the effect of hirudin on ECM deposition associated with DKD renal tubular epithelial cells and showed that hirudin had roles in renal tubular fibrosis in the rat model of DKD induced by streptozotocin and reduced high-glucose induced ECM deposition in HK-2 cells.

Several previously published studies have shown that hyperglycemia can cause renal tubular hypoxia [24]. Abnormal oxygen metabolism may be an important mechanism of renal tubular dysfunction and fibrosis [25]. Hypoxia-inducible factor-1 α (HIF-1 α) is a heterodimeric transcription factor that participates in the adaptive response to reduced oxygen tension in hypoxic cells and is an important regulator of cellular oxygen

metabolism, glucose transport, and cell apoptosis [25]. Transient hypoxia and HIF-1 α pathway activation promote tissue repair, but in chronic injury, chronic hypoxia, and pathological tissue repair, the HIF-1 α pathway may lead to fibrosis, and long-term overexpression of HIF-1 α may eventually promote organ fibrosis [26]. In DKD and renal tubular hypoxia, HIF-1 α rapidly deposits in the cells and promotes the expression of vascular endothelial growth factor (VEGF) and its receptor VEGF-R2. VEGF, also known as vascular permeability factor, is a specific mitogen that promotes endothelial cell survival, proliferation, and migration. Cell proliferation can increase endothelial cell permeability and regulate the ECM. The HIF-1 α /VEGF signaling pathway has previously been shown to be involved in the regulation of the ECM [25]. Hirudin has previously been shown to affect the expression of HIF-1 α /VEGF, while the HIF-1 α /VEGF pathway regulates the accumulation of ECM [27]. The findings from the present study are supported by these previous studies and showed that hirudin reduced the deposition of ECM in the rat model of DKD through inhibition of the HIF-1 α /VEGF pathway to protect kidney function and delay disease progression.

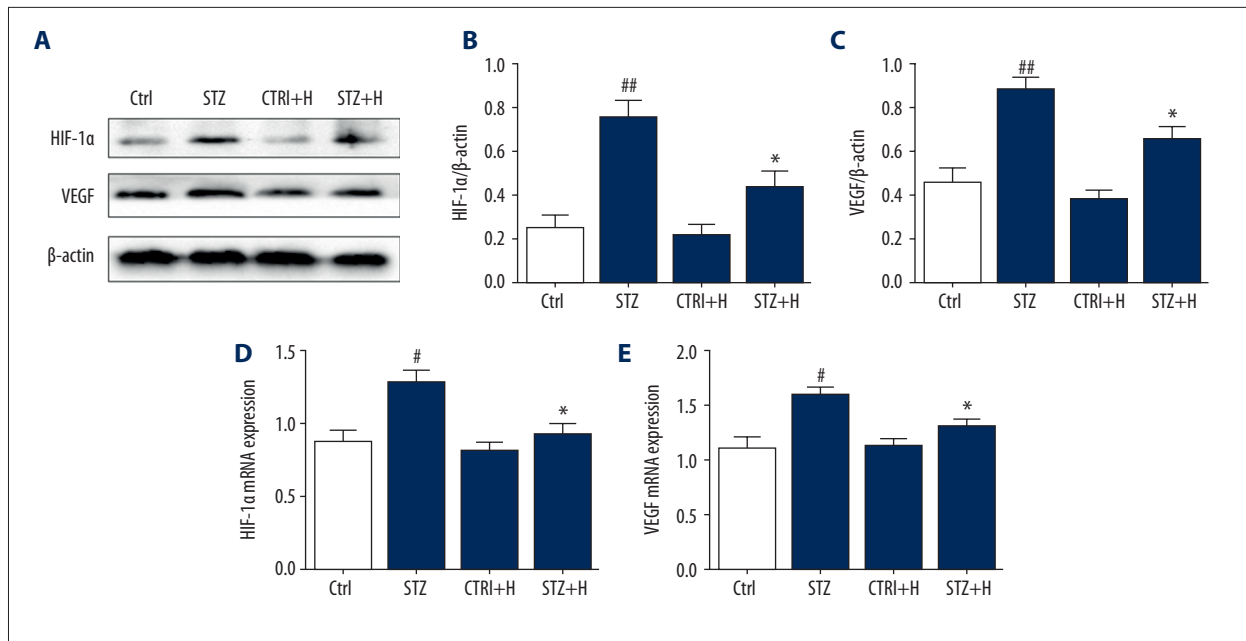


Figure 4. The effect of hirudin on the hypoxia-inducible factor-1 α (HIF-1 α)/vascular endothelial growth factor (VEGF) signaling pathway in the rat model of diabetic kidney disease (DKD). **(A)** The protein expression levels of HIF-1 α and VEGF were determined using Western blot. **(B, C)** Quantification of protein expression was performed using GraphPad Prism version 7.0. β -actin was used as an internal control. The gray value was evaluated and calculated by qualitatively. **(D, E)** The relative mRNA levels of HIF-1 α and VEGF were evaluated using quantitative real-time polymerase chain reaction (qRT-PCR). All data are expressed as the mean \pm standard deviation (SD). Compared with the normal control group, ^{##} $P < 0.01$; [#] $P < 0.05$. Compared with the model group, ^{**} $P < 0.01$; ^{*} $P < 0.05$. Ctrl – control; STZ – streptozotocin; DKD – diabetic kidney disease; H – hirudin; FN – fibronectin; IV-C – type IV collagen; HIF-1 α – hypoxia-inducible factor-1 α ; VEGF – vascular endothelial growth factor; Ctrl+H – normal control+hirudin group; STZ+H – STZ+hirudin group.

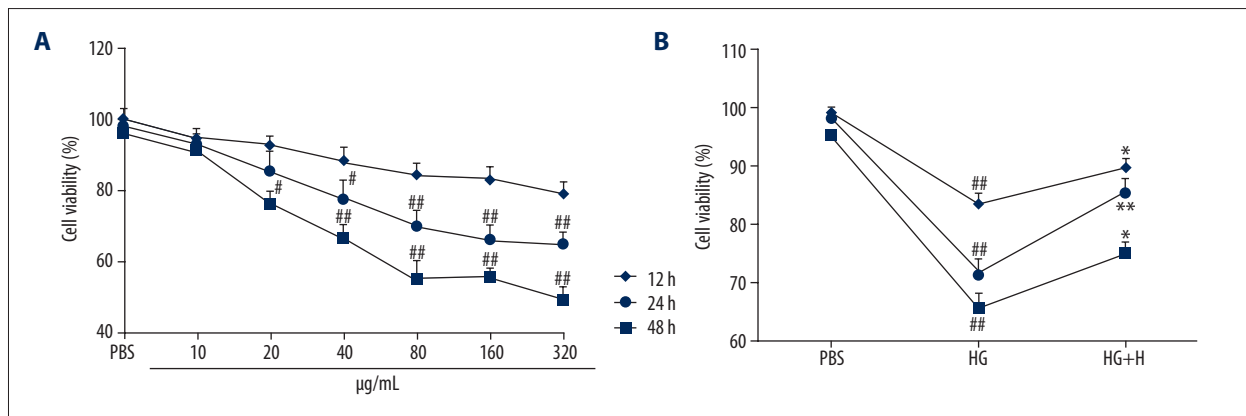


Figure 5. The effects of hirudin on the proliferation of HK-2 cells. **(A)** Cells were treated respectively with PBS (control), hirudin (10, 20, 40, 80, 160, and 320 μ g/mL) for 12, 24, and 48 hours. The Cell Counting Kit-8 (CCK-8) assay was used to detect cell viability. [#] $P < 0.05$; ^{##} $P < 0.01$ vs. control. **(B)** Cells were treated with PBS (control), HG, hirudin 10 μ g/mL+HG (H+HG) for 12, 24, and 48 hours. The viability of cells was measured by the CCK-8 assay. PBS – phosphate-buffered saline; HG – high glucose; H – hirudin; CCK-8 – Cell Counting Kit-8. Compared with the control group, ^{##} $P < 0.01$; [#] $P < 0.05$. Compared with the model group, ^{**} $P < 0.01$, ^{*} $P < 0.05$. PBS – control group; HG – high-glucose culture group; HG+H – high glucose+hirudin group.

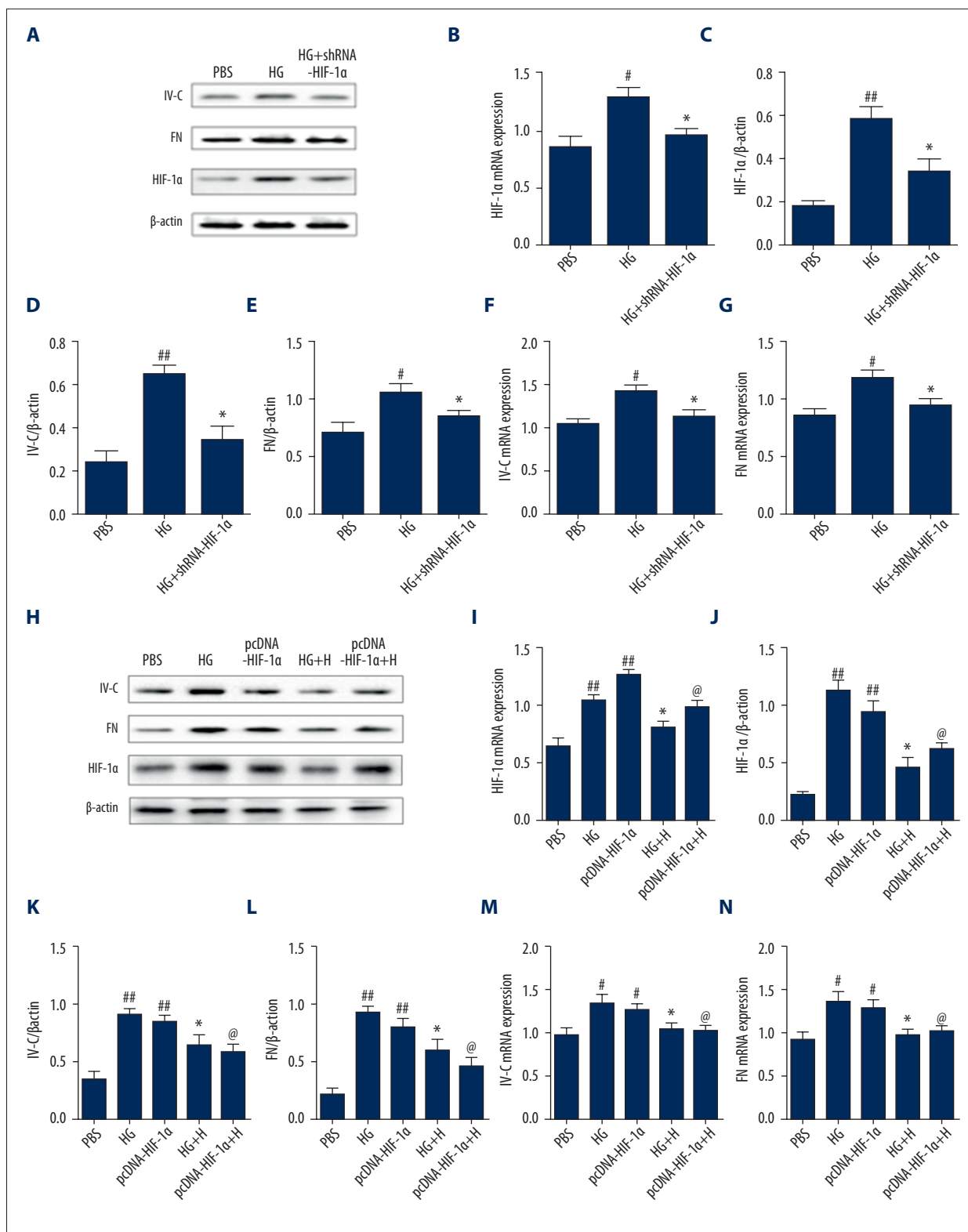


Figure 6. Hirudin reduced the expression of fibronectin and type IV collagen in HK-2 cells induced by high glucose through inhibition of the hypoxia-inducible factor-1α (HIF-1α)/vascular endothelial growth factor (VEGF) pathway. Changes in type IV collagen and fibronectin after HIF-1α knockout. **(A)** The protein expression levels of type IV collagen and fibronectin were determined using Western blot. **(B, C)** The relative mRNA and protein expression levels of HIF-1α were evaluated using

quantitative real-time polymerase chain reaction (qRT-PCR) and Western blot. (D, E) Quantification of protein expression was performed using GraphPad Prism version 7.0. β -actin was used as an internal control. The gray value was evaluated and calculated by qualitatively. (F, G) The relative mRNA levels of type IV collagen and fibronectin were evaluated using qRT-PCR. Changes in type IV collagen and fibronectin expression after overexpression of HIF-1 α and intervention with hirudin. (H) The protein expression levels of type IV collagen and fibronectin were determined using Western blot. (I, J) The relative mRNA and protein expression levels of HIF-1 α was evaluated using qRT-PCR. (K, L) GraphPad Prism software was used for quantitative analysis of protein expression. β -actin was used as an internal control. The gray value was evaluated and calculated qualitatively. (M, N) The relative mRNA levels of type IV collagen and fibronectin were evaluated using qRT-PCR. All data are expressed as the mean \pm standard deviation (SD). Compared with the control group, $^{###}$ $P < 0.01$; $^{\#}$ $P < 0.05$; Compared with the model group, ** $P < 0.01$; * $P < 0.05$; Compared with pCDNA-HIF-1 α , $^{\circ}$ $P < 0.05$. H – hirudin; HG – high-glucose; FN – fibronectin; IV-C – type IV collagen; HIF-1 α – hypoxia-inducible factor-1 α ; PBS – control group; HG+H – high glucose+hirudin group; HG+shRNA-HIF-1 α – high glucose+HIF-1 α knockout group; pCDNA-HIF-1 α – HIF-1 α overexpression group; pCDNA-HIF-1 α +H – HIF-1 α overexpression+hirudin group.

Conclusions

This study aimed to investigate the effect of hirudin on the production of extracellular matrix (ECM) factors by renal tubular epithelial cells in a rat model of diabetic kidney disease (DKD) and in HK-2 normal human renal tubule epithelial cells. Hirudin suppressed the expression of ECM markers by inhibiting the hypoxia-inducible factor-1 α (HIF-1 α) and vascular endothelial growth factor (VEGF) signaling pathway in renal tubular epithelial cells in DKD.

References:

- Ahmad J: Management of diabetic nephropathy: Recent progress and future perspective. *Diabetes Metab Syndr*, 2015; 9(4): 343–58
- Hu C, Sun L, Xiao L et al: Insights into the mechanisms involved in the expression and regulation of extracellular matrix proteins in diabetic nephropathy. *Curr Med Chem*, 2015; 22(24): 2858–70
- Lu Z, Zhong Y, Liu W et al: The Efficacy and mechanism of Chinese herbal medicine on diabetic kidney disease. *J Diabetes Res*, 2019; 2019: 2697672
- Muskiet M, Wheeler DC, Heerspink H: New pharmacological strategies for protecting kidney function in type 2 diabetes. *Lancet Diabetes Endocrinol*, 2019; 7(5): 397–412
- Koszegi S, Molnar A, Lenart L et al: RAAS inhibitors directly reduce diabetes-induced renal fibrosis via growth factor inhibition. *J Physiol*, 2019; 597(1): 193–209
- Liu Y: Renal fibrosis: New insights into the pathogenesis and therapeutics. *Kidney Int*, 2006; 69(2): 213–17
- Zhang Y, Chen Xi W: [Research progress of TGF- β and tubulointerstitial fibrosis.] *Journal of Guangdong Medical College*, 2005; 2: 218–20 [in Chinese]
- Pang XX, Tong Y, Li HP et al: [Research progress of traditional Chinese medicine leech and its extracts in the treatment of diabetic nephropathy.] *Guangming Zhongnian*, 2019; 34(01): 168–71 [in Chinese]
- Yu C, Wang W, Jin X: Hirudin protects Ang II-induced myocardial fibroblasts fibrosis by inhibiting the extracellular signal-regulated kinase1/2 (ERK1/2) pathway. *Med Sci Monit*, 2018; 24: 6264–72
- Tang F, Hao Y, Zhang X et al: Effect of echinacoside on kidney fibrosis by inhibition of TGF-beta1/Smads signaling pathway in the db/db mice model of diabetic nephropathy. *Drug Des Devel Ther*, 2017; 11: 2813–26
- Mao Q, Chen C, Liang H et al: Astragaloside IV inhibits excessive mesangial cell proliferation and renal fibrosis caused by diabetic nephropathy via modulation of the TGF-beta1/Smad/miR-192 signaling pathway. *Exp Ther Med*, 2019; 18(4): 3053–61
- Peng L, Pan X, Yin G: Natural hirudin increases rat flap viability by anti-inflammation via p38/NF-kappaB pathway. *Biomed Res Int*, 2015; 2015: 597264
- Zhu Y, Wang J, Meng X et al: A positive feedback loop promotes HIF-1 α stability through miR-210-mediated suppression of RUNX3 in paraquat-induced EMT. *J Cell Mol Med*, 2017; 21(12): 3529–39
- Tesch GH: Diabetic nephropathy – is this an immune disorder? *Clin Sci*, 2017; 131(16): 2183–99
- Thomas MC, Cooper ME, Zimmet P: Changing epidemiology of type 2 diabetes mellitus and associated chronic kidney disease. *Nat Rev Nephrol*, 2016; 12(2): 73–81
- Parving HH, Persson F, Rossing P: Microalbuminuria: A parameter that has changed diabetes care. *Diabetes Res Clin Pract*, 2015; 107(1): 1–8
- Tessari P: Nitric oxide in the normal kidney and in patients with diabetic nephropathy. *J Nephrol*, 2015; 28(3): 257–68
- Thethi TK, Batuman V: Challenging the conventional wisdom on diabetic nephropathy: Is microalbuminuria the earliest event? *J Diabetes Complications*, 2019; 33(3): 191–92
- Zeni L, Norden A, Cancarini G et al: A more tubulocentric view of diabetic kidney disease. *J Nephrol*, 2017; 30(6): 701–17
- Chen N, Hao J, Duan HJ: [Signal pathway and extracellular matrix deposition of renal tubules in diabetic nephropathy.] *Journal of Hebei Medical University*, 2018; 39(02): 231–35 [in Chinese]
- Zhou D, Fu HY: [Production, remodeling and renal fibrosis of extracellular matrix.] *Jinagsu Medical Journal*, 2015; 41(08): 936–38 [in Chinese]
- Bi L M, Chen YL, Lu W: [Progress in the application of mink preparation in kidney disease.] *Chinese Journal of Integrated Traditional and Western Medicine on Nephrology*, 2016; 17(04): 374–76
- Fan L, Dong ZH, Yang HX et al: [Mechanism of hirudin in relieving human renal tubular epithelial fibrosis via JAK/STAT3 signaling pathway.] *Chinese Traditional Medicine*, 2018; 41(04): 982–85 [in Chinese]
- Mimura I, Nangaku M: The suffocating kidney: Tubulointerstitial hypoxia in end-stage renal disease. *Nat Rev Nephrol*, 2010; 6(11): 667–78
- Ando A, Hashimoto N, Sakamoto K et al: Repressive role of stabilized hypoxia inducible factor 1 α expression on transforming growth factor beta-induced extracellular matrix production in lung cancer cells. *Cancer Sci*, 2019; 110(6): 1959–73
- Darby IA, Hewitson TD: Hypoxia in tissue repair and fibrosis. *Cell Tissue Res*, 2016; 365(3): 553–62
- Zhou HJ, Tang T, Cui HJ et al: Thrombin-triggered angiogenesis in rat brains following experimental intracerebral hemorrhage. *J Neurosurg*, 2012; 117(5): 920–28

Conflict of interest

None.